The Puf RNA-binding proteins FBF-1 and FBF-2 inhibit the expression of synaptonemal complex proteins in germline stem cells

Christopher Merritt and Geraldine Seydoux*

SUMMARY

FBF-1 and FBF-2 (collectively FBF) are two nearly identical Puf-domain RNA-binding proteins that regulate the switch from mitosis to meiosis in the *C. elegans* germline. In germline stem cells, FBF prevents premature meiotic entry by inhibiting the expression of meiotic regulators, such as the RNA-binding protein GLD-1. Here, we demonstrate that FBF also directly inhibits the expression of structural components of meiotic chromosomes. HIM-3, HTP-1, HTP-2, SYP-2 and SYP-3 are components of the synaptonemal complex (SC) that forms between homologous chromosomes during meiotic prophase. In wild-type germlines, the five SC proteins are expressed shortly before meiotic entry. This pattern depends on FBF binding sites in the 3′ UTRs of the SC mRNAs. In the absence of FBF or the FBF binding sites, SC proteins are expressed precociously in germline stem cells and their precursors. SC proteins aggregate and SC formation fails at meiotic entry. Precocious SC protein expression is observed even when meiotic entry is delayed in *fbf* mutants by reducing GLD-1. We propose that parallel regulation by FBF ensures that in wild-type gonads, meiotic entry is coordinated with just-in-time synthesis of synaptonemal proteins.

KEY WORDS: Germ cells, Meiosis, Post-transcriptional regulation, *C. elegans*

INTRODUCTION

A crucial step in the development of the germline is the transition from an undifferentiated germ cell that divides by mitosis to a differentiating germ cell that is ready to begin meiosis. In animals, this transition often takes place via an intermediate cell type that still divides by mitosis but has begun to express factors required for meiosis. For example, in *C. elegans* a group of ~220 mitotic germ cells are maintained throughout life at the distal end of each gonad ('mitotic zone', Fig. 1A) (Byrd and Kimble, 2009; Hubbard, 2007). The progeny of these cells differentiate in a distal-to-proximal gradient along the length of the gonad. The mitotic zone contains two cell types (Fig. 1A): distal-most cells, including the germline stem cells, which remain undifferentiated throughout the life of the animal; and proximal cells, which begin to express meiotic genes and are likely to include transit-amplifying cells and cells in meiotic S phase (Cinquin et al., 2010; Hubbard, 2007). Upon exit from the mitotic zone, cells initiate the chromosome dynamics required for meiotic pairing and synapsis ('transition zone', Fig. 1A). In preparation for this transition, proximal cells in the mitotic zone activate the expression of both regulators of meiotic entry (e.g. the RNA-binding protein GLD-1) and chromosomal proteins required for synapsis (e.g. HIM-3) (Hansen et al., 2004). The mechanisms that coordinate meiotic entry with the synthesis of meiotic chromosomal proteins are not known and are the focus of this study.

Meiotic entry is regulated by a complex network of RNA-binding proteins (Byrd and Kimble, 2009). Central to the network are FBF-1 and FBF-2, two highly similar Puf-domain RNA-binding proteins known collectively as FBF (Crittenden et al., 2002). FBF prevents premature meiotic entry in the mitotic zone at least in part by inhibiting the expression of GLD-1 (Crittenden et al., 2002). FBF and GLD-1 are expressed in roughly reciprocal patterns, with high FBF/low GLD-1 distally and low FBF/high GLD-1 proximally (Crittenden et al., 2002; Lamont et al., 2004) (Fig. 1A). FBF inhibits GLD-1 expression in distal cells via the *gld-1* 3′ UTR, which contains two predicted FBF-1 binding sites (Crittenden et al., 2002). A reporter containing the *gld-1* 3′ UTR reproduces the GLD-1 protein expression pattern (Merritt et al., 2008). Mutations that eliminate FBF-1 binding in vitro (Crittenden et al., 2002) cause the *gld-1* reporter to be expressed at an evenly high level throughout the mitotic zone (Merritt et al., 2008). Reducing the dose of GLD-1 by half is sufficient to maintain a mitotic zone in *fbf* mutants, consistent with GLD-1 promoting premature meiotic entry in the absence of FBF (Crittenden et al., 2002).

What regulates the expression of meiotic chromosomal proteins is not known. In a survey of gene expression in the germline (Merritt et al., 2008), we found that the *him-3* 3′ UTR blocks expression in distal cells in a pattern similar to that observed with the *gld-1* 3′ UTR (Fig. 1D). HIM-3 is a component of the synaptonemal complex that forms between homologous chromosomes upon entry into meiosis (Zetka et al., 1999). In this study, we demonstrate that HIM-3 and four other synaptonemal proteins are regulated by FBF. Our findings suggest that parallel regulation by FBF coordinates meiotic entry with the timely production of meiotic chromosomal proteins.

MATERIALS AND METHODS

Nematode strains

C. elegans strains (Table 1) were maintained using standard procedures (Brenner, 1974).

Transgene construction and transformation

Transgenes were constructed using the Multisite Gateway cloning system (Invitrogen) as described (Merritt et al., 2008). See Table 1 and Table S1 in the supplementary material for lists of plasmids and oligos used in this

Table 1. Transgenes and strains used in this study

3′ UTR fusions

Fusion*	Transgene	pDONRP2P3R insert (oligos used)	Strain	Genotype [plasmid]	Expression	Lines	Reference
coh-1	pie-1 prom:gfp::histone H2B:coh-1 3′utr	pCM1.189 (CM703, CM704)	JH2821	unc-119(ed3); axIs1931[pCM1.204]	Unstable	1	This study
him-3	pie-1 prom:gfp::histone H2B:him-3 3′utr	pCM5.52	JH2336	unc-119(ed3); axIs1691[pCM6.52A]	Stable	–	(Merritt et al., 2008)
him-3 M1	pie-1 prom:gfp::histone H2B:him-3 M1 3′utr	pCM1.75 (CM505, CM506)	JH2619	unc-119(ed3); axIs1847[pCM1.133]	Stable	6	This study
him-3 M2	pie-1 prom:gfp::histone H2B:him-3 M2 3′utr	pCM1.174 (CM507, CM508)	JH2571	unc-119(ed3); axIs1842[pCM1.186]	Stable	2	This study
him-3 M1M2	pie-1 prom:gfp::histone H2B:him-3 M1M2 3′utr	pCM1.96 (CM505, CM506, CM507, CM508)	JH2375	unc-119(ed3); axIs1711[pCM1.101]	Stable	3	This study
htp-1	pie-1 prom:gfp::histone H2B:htp-1 3′utr	pCM1.224 (CM735, CM736)	JH2673	unc-119(ed3); axIs1866[pCM1.237]	Stable	10	This study
htp-1 M1	pie-1 prom:gfp::histone H2B:htp-1 M1 3′utr	pCM1.248 (CM848, CM849)	JH2765	unc-119(ed3); axIs1921[pCM1.255]	Stable	2	This study
htp-2	pie-1 prom:gfp::histone H2B:htp-2 3′utr	pCM1.225 (CM737, CM738)	JH2766	unc-119(ed3); axIs1922[pCM1.252]	Stable	1	This study
htp-2 M1M2	pie-1 prom:gfp::histone H2B:htp-2 M1M2 3′utr	pCM1.250 (CM852, CM853)	JH2744	unc-119(ed3); axIs1909[pCM1.257]	Unstable	1	This study
htp-3	pie-1 prom:gfp::histone H2B:htp-3 3′utr	pCM1.90 (CM705, CM706)	JH2621	unc-119(ed3); axIs1849[pCM1.205]	Stable	6	This study
msh-5	pie-1 prom:gfp::histone H2B:msh-5 3′utr	pCM1.227 (CM741, CM742)	JH2704	unc-119(ed3); axIs1890[pCM1.242]	Stable	6	This study
puf-5	pie-1 prom:gfp::histone H2B:puf-5 3′utr	pCM5.64	JH2418	unc-119(ed3); axIs1721[pCM1.89]	Stable	–	(Merritt et al., 2008)
puf-5 M1M2	pie-1 prom:gfp::histone H2B:puf-5 M1M2 3′utr	pCM1.171 (CM686, CM687, CM688, CM689)	JH2570	unc-119(ed3); axIs1841[pCM1.185]	Stable	1	This study
rad-50	pie-1 prom:gfp::histone H2B:rad-50 3′utr	pCM1.228 (CM743, CM744)	JH2682	unc-119(ed3); axIs1875[pCM1.239]	Unstable	1	This study
rad-51	pie-1 prom:gfp::histone H2B:rad-51 3′utr	pCM1.191 (CM707, CM708)	JH2623	unc-119(ed3); axIs1851[pCM1.206]	Stable	7	This study
rec-8	pie-1 prom:gfp::histone H2B:rec-8 3′utr	pCM1.197 (CM719, CM720)	JH2730	unc-119(ed3); axIs1895[pCM1.212]	Stable	1	This study
rme-2	pie-1 prom:gfp::histone H2B:rme-2 3′utr	pCM5.51	JH2313	unc-119(ed3); axIs1670[pCM6.51B]	Stable	–	(Merritt et al., 2008)
syp-1	pie-1 prom:gfp::histone H2B:syp-1 3′utr	pCM5.53 (CM379, CM380)	JH2260	unc-119(ed3); axIs1648[pCM6.53]	Stable	3	This study
syp-2	pie-1 prom:gfp::histone H2B:syp-2 3′utr	pCM1.192 (CM709, CM710)	JH2698	unc-119(ed3); axIs1884[pCM1.207]	Stable	10	This study
syp-2 M1	pie-1 prom:gfp::histone H2B:syp-2 M1 3′utr	pCM1.235 (CM809, CM810)	JH2680	unc-119(ed3); axIs1873[pCM1.240]	Stable	19	This study
syp-3	pie-1 prom:gfp::histone H2B:syp-3 3′utr	pCM1.193 (CM711, CM712)	JH2626	unc-119(ed3); axIs1854[pCM1.208]	Stable	10	This study
syp-3 M1M2	pie-1 prom:gfp::histone H2B:syp-3 M1M2 3′utr	pCM1.247 (CM817, CM818)	JH2751	unc-119(ed3); axIs1916[pCM1.254]	Unstable	1	This study

Table 1. Continued

3′ UTR fusions

Fusion*	Transgene	pDONRP2P3R insert (oligos used)	Strain	Genotype [plasmid]	Expression	Lines	Reference
tbb-2	pie-1 prom:gfp::histone H2B:tbb-2 3′utr	pCM1.36	JH2297	unc-119(ed3); axIs1664[pCM1.34B]	Stable	–	(Merritt et al., 2008)
zhp-3	pie-1 prom:gfp::histone H2B:zhp-3 3′utr	pCM1.230 (CM747, CM748)	JH2707	unc-119(ed3); axIs1893[pCM1.243]	Stable	8	This study
zim-1	pie-1 prom:gfp::histone H2B:zim-1 3′utr	pCM1.194 (CM713, CM714)	JH2671	unc-119(ed3); axIs1864[pCM1.209]	Stable	4	This study
zim-2	pie-1 prom:gfp::histone H2B:zim-2 3′utr	pCM1.195 (CM715, CM716)	JH2629	unc-119(ed3); axIs1857[pCM1.210]	Unstable	3	This study
zim-3	pie-1 prom:gfp::histone H2B:zim-3 3′utr	pCM1.196 (CM717, CM718)	JH2672	unc-119(ed3); axIs1865[pCM1.211]	Unstable	2	This study

Heat-shock fusions

Fusion	Transgene	pDONRP2P3R insert (oligos used)	Strain	Genotype [plasmid]	Expression	Lines	Reference
histone H2B	heatshock prom (hsp16-41):gfp::histone H2B:tbb-2 3′utr	pCM1.63 (CM210, CM211, CM344, CM480)	JH2741	unc-119(ed3); axIs1906[pCM1.291]	Stable	1	This study
him-3	heatshock prom (hsp16-41):gfp::him-3 ORF:him-3 3′utr	pCM1.279 (CM875, CM378)	JH2747	unc-119(ed3); axIs1912[pCM1.301]	Stable	6	This study
htp-1	heatshock prom (hsp16-41):gfp::htp-1 ORF:htp-1 3′utr	pCM1.277 (CM873, CM736)	JH2735	unc-119(ed3); axIs1900[pCM1.286]	Stable	2	This study
syp-2	heatshock prom (hsp16-41):gfp::syp-2 ORF:syp-2 3′utr	pCM1.275 (CM870, CM710)	JH2737	unc-119(ed3); axIs1902[pCM1.289]	Stable	2	This study
syp-3	heatshock prom (hsp16-41):gfp::syp-3 ORF:syp-3 3′utr	pCM1.276 (CM871, CM712)	JH2740	unc-119(ed3); axIs1905[pCM1.290]	Stable	4	This study

ORF fusions

Fusion	Transgene	pDONRP4P1R insert (oligos used)	pDONRP2P3R insert (oligos used)	Strain	Genotype [plasmid]	Expression	Lines	Reference
him-3	pie-1 prom:gfp::him-3 ORF:him-3 3′utr	–	–	JH2120	unc-119(ed3); axIs1534 [pDR4.16]	Stable	–	(Merritt et al., 2008)
htp-1	htp-1 prom:gfp::htp-1 ORF:htp-1 3′utr	pCM1.271 (CM862, CM863)	pCM1.277 (CM873, CM736)	JH2768	unc-119(ed3); axIs1924 [pCM1.292]	Unstable	1	This study
htp-2	htp-2 prom:gfp::htp-2 ORF:htp-2 3′utr	pCM1.272 (CM864, CM865)	pCM1.278 (CM874, CM738)	JH2748	unc-119(ed3); axIs1913 [pCM1.293]	Unstable	1	This study
syp-2	syp-2 prom:gfp::syp-2 ORF:syp-2 3′utr	pCM1.270 (CM858, CM859)	pCM1.275 (CM870, CM710)	JH2769	unc-119(ed3); axIs1925 [pCM1.295]	Unstable	2	This study
syp-3	syp-3 prom:gfp::syp-3 ORF:syp-3 3′utr	pCM1.281 (CM860, CM861)	pCM1.276 (CM871, CM712)	JH2749	unc-119(ed3); axIs1914 [pCM1.296]	Stable	3	This study

Other strains

Strain	Genotype [plasmid]	Reference
JK3022	fbf-1(ok91) II	(Crittenden et al., 2002)
JK3101	fbf-2(q738) II	(Lamont et al., 2004)
JK3107	fbf-1(ok91) fbf-2(q704)/mIn1[mIs14 dpy-10(e128)] II	(Crittenden et al., 2002)

*3′ UTR fusions with mutations in predicted FBF-1 binding site elements are named M1 and/or M2 (where M1 is the 5′-most element).

study. 3′ UTR reporters contain the *pie-1* promoter (5′ entry, pCG142), GFP::histone H2B (middle entry, pCM1.35) and gene-specific 3′ UTRs (Table 1). Heat-shock fusions contain the *hsp16-41* heat shock promoter (5′ entry, pCM1.55), GFP (middle entry, pCM1.53) and gene-specific ORF::3′UTRs (3′ entry, Table 1). ORF fusions contain gene-specific promoters (5′ entry, Table 1), GFP (middle entry, pCM1.53) and gene-specific ORF::3′UTRs (3′ entry, Table 1). QuikChange site-directed mutagenesis (Stratagene) or PCR fusion was used to create FBE mutations in 3′ entry clones (for oligos used, see Table S1 in the supplementary material). FBE sites were mutated from UGURHHAU to acaRHHAU as described (Merritt et al., 2008). All transgenes contain an *unc-119* rescue fragment and were transformed into *unc-119(ed3)* worms by microparticle bombardment as described (Merritt et al., 2008; Praitis et al., 2001).

Motif search

Motifs overrepresented in the *him-3*, *htp-1*, *htp-2*, *syp-2* and *syp-3* 3′ UTRs of *C. elegans*, *C. briggsae*, *C. remanei* and *C. brenneri* were identified using Multiple Em for Motif Elicitation (MEME, http://meme.sdsc.edu) (Bailey and Elkan, 1994). Search settings were: search of given strand only; motif width, 6-50; number of motifs per sequence, any number; maximum number of motifs to find, five. The search yielded one highly significant and highly represented motif (Fig. 2A; E-value=9.5×10^{-20}, sites=26) and four less significant and rarer motifs (E-value=2.8×10^{-3}, sites=4; E-value=15, sites=7; E-value=74, sites=3; E-value=130, sites=4).

Staining of dissected gonads

Immunostaining was performed as described (Couteau et al., 2004). Synchronized *fbf-1/2/mIn1* and *fbf-1/2* L1 larvae were grown until the L4 stage, dissected and stained on the same slides. Primary antibodies used were: rabbit anti-HIM-3 at 1:200 [from Monique Zetka (Zetka et al., 1999)] and rabbit anti-HTP-1/2 at 1:200 [from Abby Dernburg (Martinez-Perez et al., 2008)]. Cy3-goat anti-rabbit (Jackson ImmunoResearch) was used as secondary antibody. FITC-conjugated anti-phospho-histone H3 (Ser10), clone 3H10 (Upstate Cell Signaling Solutions), was used at 1:50 to mark mitotic germ cells.

RNA immunoprecipitation (IP) and immunoblots

Worm lysate preparation and IPs were performed as described (Cheeseman et al., 2004), with the following modifications. Beads were washed with IP buffer (50 mM Hepes, 1 mM EGTA, 3 mM $MgCl_2$, 150 mM KCl, 10% glycerol, 0.05% NP40, pH 7.4) containing protease inhibitors and antibody-coupled beads were blocked with BSA and heparin in IP buffer prior to use. Worms were grown using plates instead of liquid culture and worm lysates were pre-absorbed against empty beads. RNA was eluted with 0.1 M glycine (pH 2.5) and isolated in TRIZOL. Protein was eluted with 2× SDS-PAGE loading buffer. A detailed IP protocol is available upon request.

Primary antibodies for western blots were Living Colors anti-GFP A. v. monoclonal antibody (JL-8) (Clontech) at 1:1000, and anti-α-tubulin monoclonal antibody produced in mouse (clone DM1A) (Sigma) used at 1:1000. Secondary antibodies used for western blots were HRP-goat anti-mouse IgG1a and IgG2a (Jackson ImmunoResearch), both used at 1:5000.

Quantitative RT-PCR (qPCR)

Bound RNA from IPs was extracted in TRIZOL, eluted in water, treated with Turbo DNase (Ambion), and converted to cDNA using the iScript cDNA Synthesis Kit (Bio-Rad). qPCR was performed using SYBR Green and an iCycler thermocycler (Bio-Rad) with the iQ5 Multicolor Real-Time PCR Detection System (Bio-Rad). PCR primer pairs were designed with at least one primer spanning an exon junction and PCR primer pair efficiencies were determined for use in the final quantification of fold change. PCR primers were also tested to assure that no primer dimers were formed in the qPCR reaction. Each qPCR reaction contained: 8.7 μl water, 10 μl 2× iQ SYBR Green Supermix (Bio-Rad), 0.4 μl sense primer at 20 μM, 0.4 μl antisense primer at 20 μM, and 0.5 μl of cDNA (this allowed for at least 80 qPCR reactions per IP). Cycling protocol was: 95°C for 5 minutes (denaturation); 95°C for 15 seconds, 60°C for 1 minute (46 times, amplification and quantification); 95°C for 1 minute, 55°C for 1 minute; 55-95°C for 15 seconds (81 times, melting curve); 4°C hold (cooling). For all qPCR reactions, melting curves of final PCR products were determined to ensure a single product and no primer dimers. All qPCR reactions were performed in triplicate, Ct values were determined with iQ5 Optical System Software (Bio-Rad) and fold change was determined using Pfaffl's method (Pfaffl, 2001): $E_{target}^{\Delta Ct\ target\ (anti-GFP\ IP-IgG\ IP)}/E_{actin}^{\Delta Ct\ actin\ (anti-GFP\ IP-IgG\ IP)}$. Error bars represent standard error.

RNAi

RNAi was performed by feeding as described (Merritt et al., 2008), using the empty feeding L4440 (a gift from Andy Fire, available at www.addgene.org) as a negative control. *fbf-1/2*, *mex-3*, *him-3* and *syp-2* RNAi feeding constructs were obtained from the Ahringer RNAi Feeding Library (Kamath et al., 2003). Worms were fed RNAi bacteria on NGM plates containing 1 mM IPTG and 100 μg/ml ampicillin. For RNAi of adults with 3′ UTR reporters (Fig. 3A and see Fig. S2 and Table S2 in the supplementary material), L4 larvae were fed for either 12 hours (*fbf-1/2*) or 18 hours (L4440 and *mex-3*). Hermaphrodites treated for only 12 hours with *fbf-1/2* RNAi retain a mitotic zone (Merritt et al., 2008). For *fbf-1/2* and *gld-1* RNAi of adults with GFP::ORF fusions, L1 larvae were fed for 60 hours or longer (to adult stage) (Fig. 6B and see Fig. S4B in the supplementary material). For *fbf-1/2* RNAi feeding of L2 and L4 stage animals (Fig. 3B, Fig. 5A,B, Fig. 6A and see Fig. S3 in the supplementary material), L1 larvae were fed for 24 hours (to L2 stage) or for 40 hours (L4 stage).

Microscopy

For whole adult gonads (see Fig. S1 in the supplementary material), images were acquired at 400× with a CoolSNAP HQ digital camera (Photometrics) attached to a Zeiss AX10 microscope. Images were acquired and normalized linearly with IPLab software (Scanalytics). All other images were acquired at 400× (except 1000× for Fig. 6A) with a Cascade QuantEM:512 SC camera attached to a CSUX-A1 spinning-disc confocal system (Yokogawa Electric) mounted to a Zeiss imager Z1. An L23 405-50 mW, 491-50 mW, 561-50 mW LaserStack laser system (Intelligent Imaging Innovations) was used for illumination. Images were acquired and normalized linearly with Slidebook (Intelligent Imaging Innovations). Images were taken in a single focal plane for GFP::histone H2B strains and somatic heat-shock GFP::ORF strains (Fig. 1, Fig. 3, Fig. 5C and see Figs S1-S3 in the supplementary material). Images were taken in a single focal plane (Fig. 6B) or as collapsed *z*-stacks for germline GFP::ORF strains and antibody staining (Fig. 5A,B, Fig. 6A and see Fig. S4B in the supplementary material). Normalization for all images was performed with the intensity of the non-worm background area set to black and the brightest germline GFP signal set to white. Normalized images were imported and saved as .tiff files in Photoshop CS2 (Adobe).

RESULTS

3′ UTRs from *htp-1*, *htp-2*, *syp-2* and *syp-3* are sufficient to downregulate gene expression in germline progenitors

To determine whether meiotic proteins depend on 3′ UTR sequences for regulation in the mitotic zone, we screened the 3′ UTRs from 15 *C. elegans* genes that encode proteins implicated in early meiotic chromosome dynamics (Fig. 1B). Each 3′ UTR was cloned downstream of a GFP::histone H2B germline reporter and transformed into worms by microparticle bombardment (see Materials and methods) (Fig. 1C). Four 3′ UTRs (*htp-1*, *htp-2*, *syp-2*, *syp-3*) strongly blocked reporter expression in distal-most cells (Fig. 1B). As with the *him-3* 3′ UTR, expression was first detected in the proximal half of the mitotic zone and reached peak levels in the transition zone (meiotic entry) (Fig. 1D). All other 3′ UTRs allowed some reporter expression throughout the mitotic zone, including the distal-most cells (Fig. 1B). Consistent with these findings, HIM-3, HTP-1/2, SYP-2 and SYP-3 proteins have been reported to be absent from distal-most cells, whereas HTP-3, RAD-51, ZIM-1, ZIM-2, ZIM-3, REC-8 and COH-1 have been detected
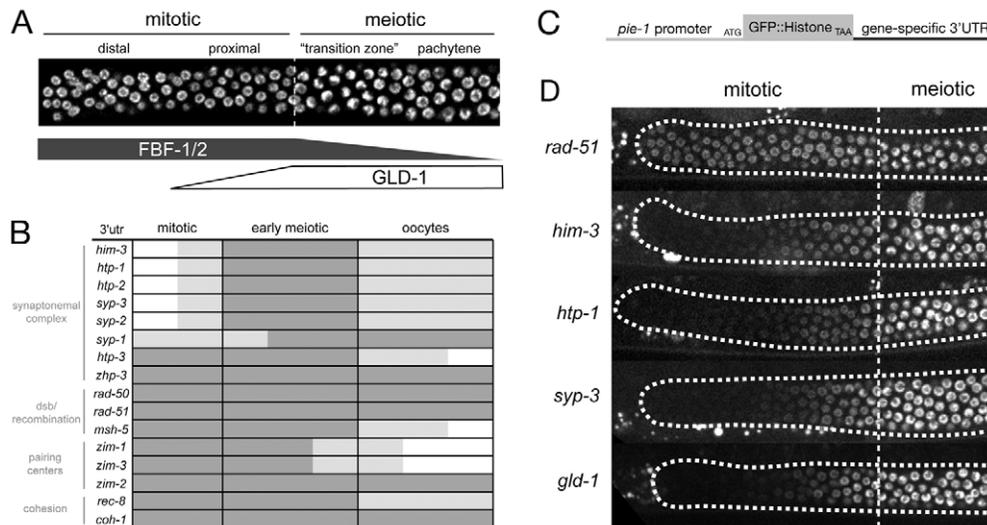
Fig. 1. Summary of 3′ UTR fusions examined in this study. (**A**) The distal end of the *C. elegans* adult gonadal tube. Development proceeds from distal (left) to proximal (right). The transition zone where germ cells initiate meiotic prophase is characterized by a distinct crescent chromosomal morphology and is marked by a vertical dashed line in this and all other figures. The proximal half of the 'mitotic zone' includes cells that have initiated meiotic S phase (reviewed by Hubbard, 2007). (**B**) Expression patterns of the 3′ UTR reporters examined in this study. Genes are arranged by functional class. Dark gray indicates the strongest domain(s) of GFP::histone H2B expression, light gray indicates weaker domain(s) of GFP expression, and white indicates no GFP expression. (**C**) The design of the 3′ UTR fusions. The *pie-1* promoter is permissive for expression in all germ cells (Merritt et al., 2008). GFP::histone H2B provides the protein reporter. (**D**) Expression of selected 3′ UTR reporters in the distal end of the gonad. The gonad is outlined.

throughout the mitotic zone (Colaiacovo et al., 2003; Goodyer et al., 2008; Pasierbek et al., 2001; Phillips and Dernburg, 2006). The only exceptions were RAD-50 and MSH-5 (no antibody staining reported) and SYP-1 and ZHP-3. SYP-1 and ZHP-3 are absent from distal-most cells (Bhalla et al., 2008; MacQueen et al., 2002), but showed an even level of expression throughout the mitotic zone in our reporter assay. The *syp-1* 3′ UTR reporter was expressed at a moderate level in the mitotic zone and was upregulated in mid-pachytene (see Fig. S1 in the supplementary material), raising the possibility that this 3′ UTR is at least partially inhibited in distal germ cells (see Discussion).

We conclude that although 3′ UTR regulation may not be sufficient to account for the distribution of all meiotic proteins, a subset of meiotic 3′ UTRs is sufficient to suppress expression in the mitotic zone. Interestingly, all five proteins in this subset are components of the synaptonemal complex (SC), the zipper-like structure that links homologous chromosomes. HIM-3, HTP-1 and HTP-2 are HORMA-domain proteins that localize to the lateral elements of the SC, whereas SYP-2 and SYP-3 are coiled-coil-domain proteins that localize to the central region of the SC (reviewed by Mlynarczyk-Evans and Villeneuve, 2010). We refer to *him-3*, *htp-1*, *htp-2*, *syp-2* and *syp-3* collectively as SC genes.

FBF activity and FBF binding sites are required to silence SC 3′ UTR reporters in the mitotic zone

To determine whether the SC genes are co-regulated, we searched for a sequence shared among the 3′ UTRs of the SC genes and their homologs in three other nematode species (*C. briggsae*, *C. remanei* and *C. brenneri*). Using MEME (see Materials and methods), we identified the motif UCnUGUnnnAU (Fig. 2A). This motif (Fig. 2B, blue boxes) is present in one or more copies in all the *C. elegans* SC 3′ UTRs with the exception of *syp-2*, which has two versions of the motif missing the first U (CCUUGUUUUAU, ACAUGUAUCAU)

(conserved bases underlined; data not shown). UCnUGUnnnAU matches the FBF-response element (FBE) in the *fem-3* 3′ UTR, a known FBF target (Crittenden et al., 2002; Zhang et al., 1997). UGUnnnAU is the minimal sequence required for FBF binding in vitro (Bernstein et al., 2005), and the preferred in vitro-defined FBF-1 binding site is UGURHHAU (R is A or G, and H is A, C or U) (Fig. 2B, red boxes) (Bernstein et al., 2005; Lee et al., 2006).

To test whether the SC 3′ UTRs are regulated by FBF, we first examined all reporters in adult hermaphrodites treated for 12 hours with *fbf-1/2* RNAi. In all cases, the 3′ UTR reporters were derepressed in the mitotic zone (Fig. 3A; see Fig. S2 and Table S2 in the supplementary material).

To control for specificity, we also examined two other 3′ UTRs that block expression in the same region of the distal gonad (*rme-2*) or in a broader region that includes part of the pachytene zone (*puf-5*) (Merritt et al., 2008). Neither 3′ UTR was derepressed following treatment with *fbf-1/2* RNAi (Fig. 3A; see Fig. S2 and Table S2 in the supplementary material). *rme-2* is a known target of MEX-3, another translational repressor expressed in the distal region (Ciosk et al., 2004). In *mex-3(RNAi)*, the *rme-2* 3′ UTR was derepressed in the distal region but none of the other reporters was affected (see Fig. S2 and Table S2 in the supplementary material). We conclude that the SC 3′ UTRs depend on FBF for repression, but that not all 3′ UTRs inhibited in the mitotic zone depend on FBF for regulation.

To test whether the predicted FBF-1 sites are functional, we first mutated those matching the consensus UGURHHAU (Fig. 2B, red boxes) to acaRHHAU, which does not bind FBF-1 in vitro (Bernstein et al., 2005; Lee et al., 2006). Such mutations were sufficient to derepress the *him-3*, *htp-1*, *htp-2* and *syp-2* 3′ UTR reporters throughout the mitotic zone (Fig. 3A). To derepress the *syp-3* 3′ UTR reporter, it was necessary to also mutate a nearby motif (UCAUGUCGAAU) that does not match the in vitro-defined

Fig. 2. Conserved motifs in the 3′ UTRs of synaptonemal complex (SC) genes and their homologs. (**A**) Conserved motif found in the SC 3′ UTRs by MEME (see Materials and methods). (**B**) Shown are sites matching the MEME motif (blue boxes, UCNUGUNNNAU), sites matching the in vitro-defined preferred FBF-1 binding site (red boxes, UGU A/G A/C/U A/C/U AU) (Bernstein et al., 2005), and sites matching both (red and blue boxes) in SC 3′ UTRs from *C. elegans*, *C. briggsae*, *C. remanei* and *C. brenneri*. Asterisks denote sites mutated (from UGUNNNAU to acaNNNAU) in reporters shown in Fig. 3. Red asterisks denote sites unambiguously required for repression by FBF. Sites in *him-3* were mutated singly (data not shown) and in combination (see Fig. 3); mutation in the first site was sufficient for full derepression (data not shown). The second site in *syp-3* was mutated singly and had no effect (data not shown), whereas the first site in *syp-3* was mutated in combination with the second site and found to cause derepression (see Fig. 3). (**C**) Alignment of sites required for repression in the SC 3′ UTRs (red asterisks in B) and in the *fem-3* 3′ UTR (Ahringer and Kimble, 1991). A 5′ cytosine is conserved in all (purple). The *syp-3* site has two bases (orange) that do not fit the in vitro-defined FBF-1 binding site. Note that all sites, except for *syp-2*, also have a uracil before the conserved 5′ cytosine. The repressive FBF-response element (FBE) consensus is based on all the sequences shown here (see Discussion).

FBF-1 consensus at positions 4 and 5, but which matches the MEME motif (Fig. 2B, blue box). The *puf-5* 3′ UTR contains two predicted FBF-1 binding sites (data not shown), but mutations in these sites did not affect expression of the *puf-5* reporter, consistent with the observation that this reporter is not affected in *fbf-1/2(RNAi)* (Fig. 3A). We conclude that the SC 3′ UTRs depend on predicted FBF-1 binding sites (or related sites) for repression, but that not all predicted FBF-1 sites are essential for regulation.

FBF activity and FBF binding sites are required to silence SC 3′ UTR reporters in germline progenitors

Our results so far show that FBF is required to inhibit SC reporter expression in the distal mitotic zone of adult hermaphrodites, which includes the germline stem cells. To determine whether FBF also functions in the progenitors of the germline stem cells, we examined the SC 3′ UTR reporters in L2 larvae. At this stage, all germ cells are proliferating and none have initiated meiosis. Wild-type SC 3′ UTR constructs were not expressed at this stage (Fig. 3B). By contrast, the SC 3′ UTR constructs with mutations in the

predicted FBF sites were expressed in all L2-stage germ cells (Fig. 3B). Expression was also seen in all cells when wild-type SC 3′ UTR constructs were examined in hermaphrodites that were double mutant for *fbf-1* and *fbf-2* [*fbf-1(ok91);fbf-2(q704)*] or hermaphrodites treated with *fbf-1/2* RNAi from the L1 stage (Fig. 3B). We conclude that FBF is required both in adult germline stem cells and in their larval progenitors to block the expression of SC 3′ UTR reporters.

FBF-1 and FBF-2 function redundantly to repress the *him-3* 3′ UTR

FBF-1 and FBF-2 function redundantly, but also have unique functions (Crittenden et al., 2002; Lamont et al., 2004). To determine whether FBF-1 and FBF-2 function redundantly to regulate the SC genes, we compared expression of the *him-3* 3′ UTR reporter in mutants lacking FBF-1 [*fbf-1(ok91)*], FBF-2 [*fbf-2(q738)*], or both [*fbf-1(ok91);fbf-2(q704)*]. We examined early L4 larvae because at this stage all three genotypes have a normal mitotic zone. We observed weak derepression of the *him-3* reporter in the mitotic zone of *fbf-1(ok91)* larvae, no derepression in *fbf-*
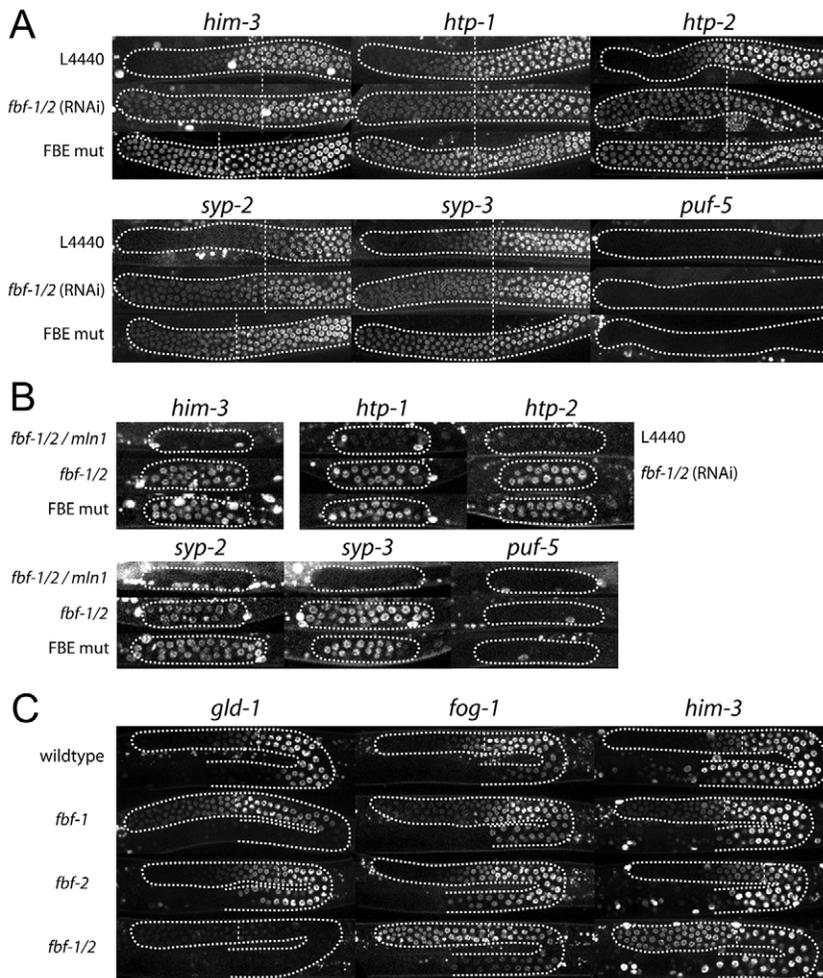
Fig. 3. FBF and predicted FBF binding sites are required for downregulation of SC 3' UTR reporters in the mitotic zone. (**A**) Fluorescence photomicrographs of distal arms from *C. elegans* adult hermaphrodites expressing the indicated 3' UTR fusions, and fed bacteria containing either the empty feeding vector (L4440), the *fbf-1* and *fbf-2* feeding vectors [*fbf-1/2(RNAi)*], or no vector (FBE mutant). FBE mutants are the 3' UTR reporters mutated at the predicted FBF sites shown in Fig. 2. See Table S2 and Fig. S2 in the supplementary material for numbers and additional 3' UTR fusions examined. (**B**) Fluorescence photomicrographs of L2 gonadal arms expressing the indicated 3' UTR reporters and treated as in A. In the case of *him-3*, *syp-2*, *syp-3* and *puf-5*, the 3' UTR reporter fusions were examined in hermaphrodites heterozygous (*fbf-1/2/mIn1*) or homozygous (*fbf-1/2*) for mutations in *fbf-1* and *fbf-2* [*fbf-1(ok91);fbf-2(q704)*]. (**C**) Fluorescence photomicrographs of L4 gonads expressing the indicated 3' UTR fusions in *fbf-1(ok91)*, *fbf-2(q738)* and *fbf-1(ok91);fbf-2(q704)* mutant larvae. Note that in all cases, moderate derepression of the transgenes is observed in the *fbf-1* single mutant but not in the *fbf-2* single mutant, suggesting that FBF-1 is only partially redundant with FBF-2 in this assay.

2(q738) larvae, and complete derepression in the *fbf-1(ok91);fbf-2(q704)* double mutant (Fig. 3C). We conclude that FBF-1 and FBF-2 function redundantly to inhibit *him-3*.

gld-1 and *fog-1*, two well-characterized FBF targets (Crittenden et al., 2002; Thompson et al., 2005), behaved similarly to *him-3*, except that the *gld-1* 3' UTR reporter was expressed only very weakly in *fbf-1;fbf-2* larvae (Fig. 3C). This result is consistent with the fact that GLD-1 is expressed at low levels in sperm-producing germlines (Jones et al., 1996) and with the analyses of Suh et al. (Suh et al., 2009), who proposed that FBF is required both to repress and activate *gld-1* (Suh et al., 2009). FBF-dependent activation, however, is unlikely to be a characteristic of all FBF targets, as the *him-3*, *fog-1*, *syp-2* and *syp-3* reporters were all strongly expressed in *fbf-1(ok91);fbf-2(q704)* hermaphrodites (Fig. 3C and see Fig. S3 in the supplementary material).

FBF-1 and FBF-2 interact with SC mRNAs in vivo

The finding that FBF and its predicted binding sites are essential to repress the SC 3' UTRs suggests that FBF-1 and FBF-2 inhibit the SC mRNAs via direct binding. To test this prediction further, we examined whether FBF-1 and FBF-2 associate with the SC mRNAs in vivo. We immunoprecipitated FBF-1 and FBF-2 as GFP fusions from worm extracts (Fig. 4A). In parallel, we also immunoprecipitated GFP::tubulin as a negative control (Fig. 4A). RNA abundance in the immunoprecipitates was determined by quantitative real-time PCR (qRT-PCR), and expressed as a ratio over

RNA immunoprecipitated by a control antibody (IgG). Results were normalized to the extent of *actin* mRNA enrichment in each immunoprecipitation. We found that the five SC mRNAs bound preferentially to GFP::FBF-1 and GFP::FBF-2 as compared with GFP::tubulin (Fig. 4B). Binding efficiency varied widely, with *htp-1* mRNA binding most efficiently (34.6- and 28.9-fold enrichments) and *syp-2* mRNA binding least efficiently (4.4- and 3.1-fold enrichments). *syp-1* also bound robustly to GFP::FBF-1 (18.8- and 7.4-fold enrichments). The *syp-1* 3' UTR reporter was expressed at low levels throughout the mitotic zone (Fig. 1 and see Fig. S1 in the supplementary material), raising the possibility that this mRNA might also be under FBF regulation. All mRNAs that showed strong expression throughout the mitotic zone in the 3' UTR reporter assay exhibited weak enrichment (3.3- and 2.9-fold enrichments for *zim-2*) or no significant enrichment (less than 2.1-fold). Interestingly, these mRNAs include four that contain predicted FBF-1 binding sites in their 3' UTRs (Fig. 4B). These results confirm that SC mRNAs are direct FBF targets, and suggest that not all predicted FBF-1 binding sites are recognized by FBF in vivo.

In the absence of FBF, SC proteins are expressed precociously in germline stem cells and their progenitors

To examine the distribution of the SC proteins in *fbf-1;fbf-2* mutants, we used antibodies against HIM-3 and HTP-1/2 (Martinez-Perez et al., 2008; Zetka et al., 1999), and GFP fusions
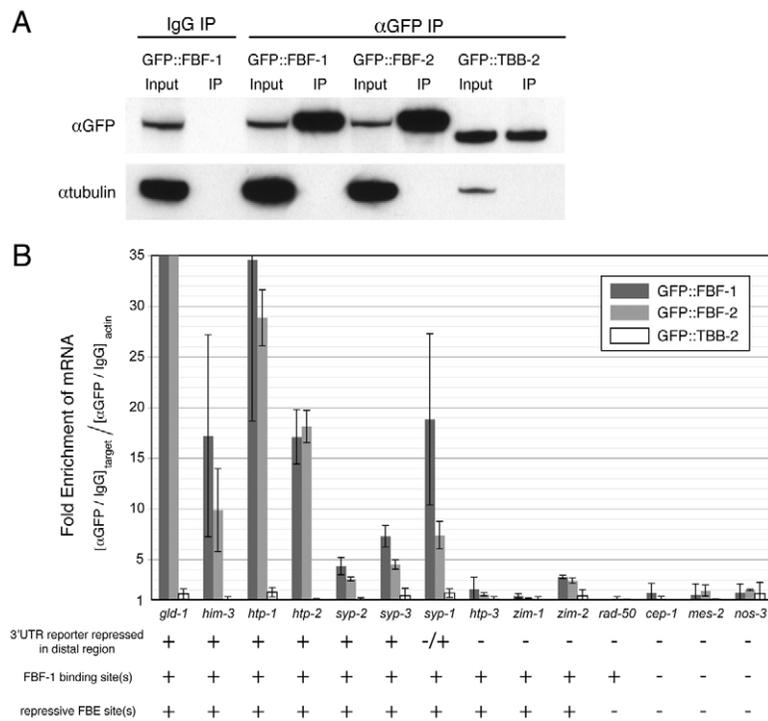
Fig. 4. FBF-1 and FBF-2 interact with endogenous SC mRNAs in vivo. (**A**) Extracts from worms expressing GFP::FBF-1, GFP::FBF-2 and GFP::TBB-2 (β-tubulin) were immunoprecipitated with either a GFP antibody or IgG. Immunoprecipitates were blotted for GFP or α-tubulin. Input is 1/16 of the immunoprecipitation (IP). (**B**) Enrichment of transcripts in GFP versus IgG immunoprecipitates. Values are normalized to *actin* mRNA enrichment to correct for non-specific binding of RNAs during the GFP IP. *gld-1* mRNA was enriched 74- and 42-fold in GFP::FBF-1 and GFP::FBF-2 IPs, respectively. Error bars represent s.e.m. FBF-1 binding sites are UGU A/G A/C/U A/C/U AU. Repressive FBE sites are CNUGU A/G/C N A/C/U AU (as in Fig. 2).

with HIM-3, HTP-1, HTP-2, SYP-2 and SYP-3 (antibodies against SYP-2 and SYP-3 were not specific enough in our hands for this analysis). In wild-type gonads, all proteins were absent from the distal half of the mitotic zone, showed increased expression through the proximal half of the mitotic zone, and were most highly expressed in the transition and pachytene regions (Fig. 5A). In the proximal half of the mitotic zone, the SC proteins were mostly nuclear and overlapped with chromatin (most evident for GFP::SYP-2 and GFP::SYP-3), but had not yet coalesced into the bright nuclear threads that are characteristic of the fully formed SCs of pachytene nuclei. We also occasionally observed GFP::SYP-2 and GFP::SYP-3 in bright nuclear puncta (Fig. 5A, arrows). These observations are consistent with previously published results (Colaiacovo et al., 2003; Martinez-Perez et al., 2008; Smolikov et al., 2007; Zetka et al., 1999) and suggest that SC proteins accumulate gradually in proximal mitotic zone cells in preparation for meiotic entry.

In *fbf-1;fbf-2* mutant or RNAi-treated gonads, we detected the SC proteins throughout the mitotic region (Fig. 5A). GFP::SC protein expression was detected as early as the L2 stage in all germ cells (Fig. 5B). As in the proximal half of the mitotic zone in wild type, the SC fusions were mainly nuclear and overlapped with chromatin, but were not yet in the bright threads characteristic of the pachytene stage. We also often observed the GFP::SC fusions in puncta (Fig. 5A,B, arrows). GFP::SC fusions also formed puncta when misexpressed in embryonic somatic cells (Fig. 5C). We conclude that FBF activity is required to inhibit premature SC protein expression in germline stem cells and their progenitors.

SC formation is defective in *fbf-1;fbf-2* mutants

As in wild type, in *fbf-1;fbf-2* mutants coalescence of the SC proteins into synaptonemal threads was observed only at meiotic entry, starting at the early L4 stage in the most proximal end of the gonad. The first ~10 nuclei to enter meiosis formed long synaptonemal threads similar to those in wild type (Fig. 6A). Later

nuclei, however, were progressively more abnormal, with stunted synaptonemal threads and large aggregates of SC proteins (Fig. 6A, arrows). Similar SYP-3 aggregates have been reported in *him-3* mutants (Smolikov et al., 2007). By the mid-L4 stage, all pachytene nuclei had an abnormal morphology in *fbf-1;fbf-2* gonads (Fig. 6A). We conclude that in *fbf-1;fbf-2* gonads, SC formation initiates at meiotic entry as in wild type but does not progress normally.

FBF-1 and FBF-2 regulate meiotic entry and SC expression independently

fbf-1;fbf-2 mutants do not maintain a mitotic zone past the L4 stage at 20°C (Crittenden et al., 2002). *fbf-1;fbf-2* adult gonads are filled with gametes that have all entered meiosis and progressed through spermatogenesis to form mature sperm (Crittenden et al., 2002). Lowering the dose of factors that promote meiosis, such as *gld-1*, can suppress this phenotype: *fbf-1;fbf-2;gld-1/+* worms maintain a mitotic zone into adulthood (Crittenden et al., 2002). We and others (T. Schedl, personal communication) have observed that *fbf-1;fbf-2* mutants grown at 25°C also maintain a mitotic zone into adulthood (see Fig. S4 in the supplementary material). To determine whether these mitotic zones misexpress SC proteins, we examined the distribution of GFP::HIM-3 in *fbf-1;fbf-2* mutants grown at 25°C and in *fbf-1;fbf-2* mutants grown at 20°C but treated with partial (incomplete) *gld-1* RNAi (Fig. 6B). We also examined GFP::SYP-3 in *fbf-1/2(RNAi)* hermaphrodites grown at 25°C (see Fig. S4 in the supplementary material). In all cases, mitotic zones were present in the adult stage and were positive for GFP::SC expression (Fig. 6B and see Fig. S4 in the supplementary material). We conclude that misregulation of SC proteins occurs in *fbf-1;fbf-2* mutants regardless of whether mitotic germ cells are fated to enter meiosis precociously.

We also tested whether reducing HIM-3 or HTP-1/2 levels could suppress the loss of a mitotic zone in *fbf-1;fbf-2* mutants. We found that, unlike *fbf-1;fbf-2;gld-1(RNAi)* hermaphrodites, *fbf-1;fbf-2;him-*
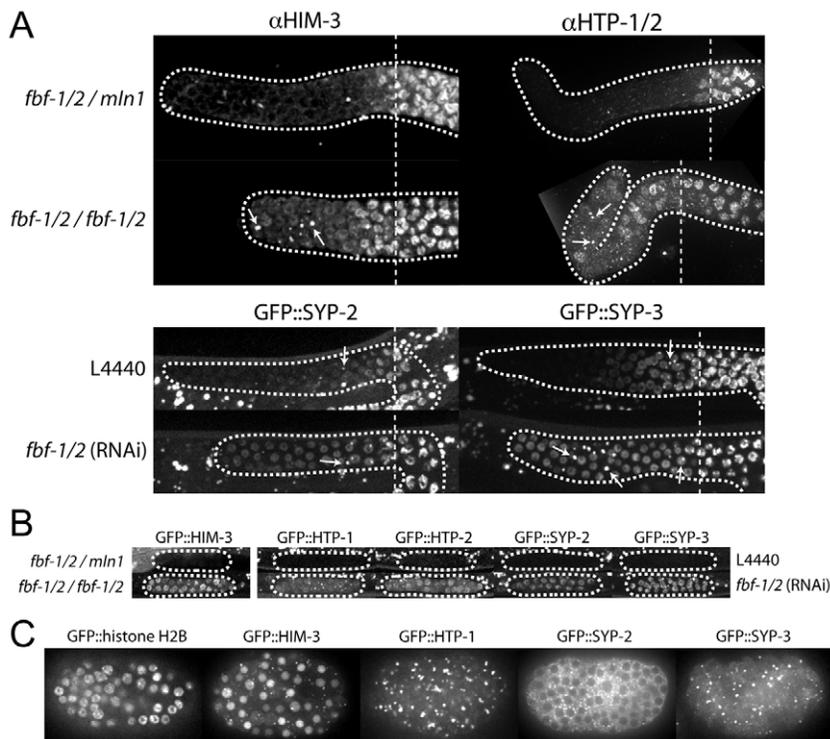
Fig. 5. Precocious expression of SC proteins in _C. elegans fbf-1;fbf-2_ mutants. (**A**) Fluorescence photomicrographs of L4 gonads. HIM-3 and HTP-1/2 expression was assessed by antibody staining (anti-HTP recognizes both HTP-1 and HTP-2) in hermaphrodites heterozygous (_fbf-1/2/mln1_) or homozygous (_fbf-1/2_) for mutations in _fbf-1_ and _fbf-2_. The HIM-3 antibody cross-reacts with mitotic spindles and other tubulin-rich structures (data not shown) and therefore some background cytoplasmic staining is visible in distal cells in the _fbf-1/2/mln1_ control. SYP-2 and SYP-3 expression was examined using GFP fusions (containing the full _syp-2_ and _syp-3_ loci) in live animals that were fed bacteria containing either the empty feeding vector (L4440) or feeding vectors for _fbf-1_ and _fbf-2_. Arrows point to aggregates. (**B**) Fluorescence photomicrographs of L2 gonadal arms expressing the indicated GFP fusions. At this stage, all germ cells are proliferating. The GFP::SC fusions are not expressed in control gonads, but are expressed in all cells in gonads lacking _fbf-1_ and _fbf-2_. (**C**) Fluorescence photomicrographs of embryos expressing the indicated GFP fusions driven by the inducible heat-shock promoter _hsp16-41_. The SC fusions form aggregates not seen with the GFP::histone H2B fusion.

3(RNAi) and _fbf-1;fbf-2;him-3(RNAi);htp-1/2(RNAi)_ hermaphrodites did not maintain a mitotic zone: all germ cells entered meiosis at the L4 stage, as seen in _fbf-1;fbf-2_ mutants [18/18 for _him-3(RNAi)_, 16/16 for _him-3;htp-1/2(RNAi)_]. We conclude that premature meiotic entry in _fbf-1;fbf-2_ mutants does not depend on HIM-3 or HTP-1/2 expression or the ability to form an SC. Consistent with these results, loss of SC proteins in wild-type gonads blocks SC formation but does not affect the timing of meiotic entry (Colaiacovo et al., 2003; Couteau and Zetka, 2005; Smolikov et al., 2007; Zetka et al., 1999). We conclude that meiotic entry and SC protein expression are not necessarily linked, and that FBF is required for their coordination.

DISCUSSION

In this study, we identify five new mRNAs regulated by FBF. The mRNAs encode components of the SC, the expression of which is inhibited by FBF in mitotic germ cells. Our results indicate that regulation by FBF ensures that SC protein synthesis is coordinated with meiotic entry.

Expression of SC mRNAs is silenced post-transcriptionally by FBF in germline stem cells and their progenitors

Four lines of evidence indicate that the SC mRNAs (_him-3_, _htp-1_, _htp-2_, _syp-2_ and _syp-3_) are direct FBF targets. First, the SC 3′ UTRs confer the same pattern of regulation in the mitotic zone as the _gld-1_ 3′ UTR: no or very low levels in distal-most cells, increasing levels in proximal cells, and high levels at the transition zone and into pachytene. Second, the SC 3′ UTRs contain one or more predicted FBF-1 binding sites, and these sites are required for repression in the mitotic zone. Third, SC mRNAs are in a complex with FBF-1 and FBF-2 in vivo. Finally, SC 3′ UTR reporters and SC proteins are expressed ectopically in all mitotic germ cells of _fbf-1;fbf-2_ mutants. Ectopic SC expression is observed as early as the L2 stage and

can be induced in adult animals by a brief exposure to _fbf-1/2_ RNAi, suggesting that FBF is required continuously to block SC expression in germline stem cells and their larval progenitors. Consistent with these observations, we previously showed that the _him-3_ promoter is active in all germ cells from the L2 stage onward (Merritt et al., 2008).

Our mutational analysis defined four sites in which mutations unambiguously caused derepression in vivo (one site each in _him-3_, _htp-2_, _syp-2_ and _syp-3_). By comparing these sites to the mutationally defined FBE in _fem-3_ (Ahringer and Kimble, 1991) and to the in vitro-defined preferred FBF-1 binding site [UGURHHAU (Bernstein et al., 2005)], we derived a 'repressive FBE' consensus (CNUGUVNHAU; Fig. 2C). The repressive FBE differs from the in vitro-defined FBF-1 binding site consensus in two ways: (1) relaxation of the middle base consensus from RHH to VNH to accommodate the _syp-3_ FBE; (2) the addition of a 5′ cytosine at the –2 position. Mutations that disrupt this cytosine in the endogenous _fem-3_ 3′ UTR (Ahringer and Kimble, 1991; Zhang et al., 1997) or in a _fem-3_ 3′ UTR reporter (C.M., unpublished) disrupt _fem-3_ regulation. Structural studies of yeast Puf3 have shown that this FBF homolog recognizes an additional 5′ cytosine in the same position relative to the core UGUNNNAU motif (Zhu et al., 2009). Consistent with a similar recognition for FBF-1, FBF-1 binding in vitro is sensitive to mutations upstream of the core element, including at the –2 position (Bernstein et al., 2005). We note that, with one exception (_syp-2_), the mutationally defined repressive FBEs also have a uracil immediately preceding the 5′ cytosine (Fig. 2C). Mutation in this base disrupts _fem-3_ regulation (Ahringer and Kimble, 1991) (C.M., unpublished), suggesting that a 5′ uracil also contributes to recognition by FBF.

Since it is based on only five mutationally defined sites, the repressive FBE consensus is unlikely to describe all sites that are functional in vivo, but it is a useful reference for prioritizing searches
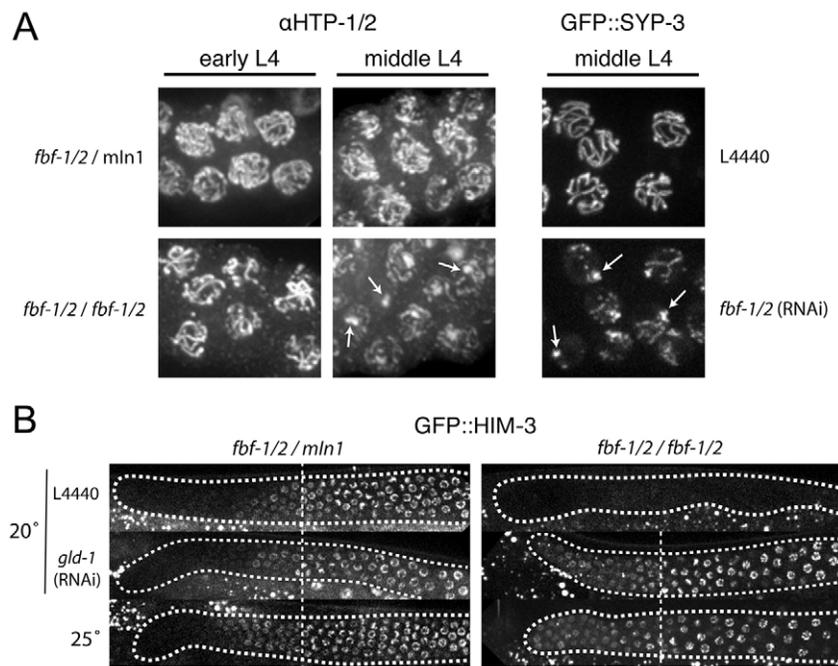
Fig. 6. Defective synaptonemal complexes in *C. elegans fbf-1;fbf-2* mutants. (**A**) Fluorescence photomicrographs of pachytene-stage germ cells in early and middle L4 gonads stained with anti-HTP-1/2 or expressing GFP::SYP-3, comparing hermaphrodites heterozygous (*fbf-1/2/mln1*) or homozygous (*fbf-1/2*) for mutations in *fbf-1* and *fbf-2* or wild-type hermaphrodites treated with control feeding vector (L4440) or *fbf-1/2* RNAi. Arrows point to representative large foci not seen in controls. (**B**) Distal gonads expressing GFP::HIM-3 in adult hermaphrodites of the indicated genotypes. All germ cells undergo spermatogenesis in *fbf-1;fbf-2* homozygotes grown at 20°C (GFP::HIM-3 is downregulated during spermatogenesis so no fluorescence is visible). *gld-1* RNAi or growth at 25°C restores a mitotic zone in *fbf-1;fbf-2* adults, but this zone still misexpresses GFP::HIM-3.

for additional new sites. A recent genome-wide microarray analysis of mRNAs immunoprecipitated by GFP::FBF-1 identified 1350 candidate FBF targets (Kershner and Kimble, 2010). This list includes the five SC mRNAs described here, and also *syp-1*, *rec-8*, *zim-2*, *rad-51* and *msh-5*, which did not behave like the SCs in the 3′ UTR reporter assay (see Table S3 in the supplementary material). With the exception of *msh-5*, all have at least one predicted FBF-1 binding site, and *syp-1* and *zim-2* have one site matching a repressive FBE. Predicted FBF-1 binding sites and repressive FBEs are overrepresented in the 3′ UTRs of meiotic genes (see Table S3 in the supplementary material), raising the possibility that most meiotic genes are in fact FBF targets. So why were only five recovered in our survey? Our 3′ UTR reporter assay might not be sensitive enough to detect the full range of FBF regulation, and some FBF targets might not be regulated in the pattern typified by *gld-1* and *him-3*. The latter might be the case for *syp-1*, which was only partially repressed in the mitotic zone (see Fig. S1 in the supplementary material), yet was enriched in the FBF-1 immunoprecipitates as robustly as *him-3* (Fig. 4). We also found some mRNAs that contained repressive FBEs but were not enriched in FBF-1 immunoprecipitates and showed no evidence of regulation in 3′ UTR reporters (*htp-3*, *zim-1* and *zhp-3*; see Table S3 in the supplementary material). Clearly, further studies are needed to define the full sequence requirements necessary for regulation by FBF.

Premature expression of SC proteins leads to aggregation and defective SC formation

Why inhibit the expression of SC proteins in immature germ cells? *fbf-1;fbf-2* mutants exhibit a defect in SC formation. Consistent with defective synapsis, *fbf-1;fbf-2* oocytes contain more than the expected six bivalents, and eggs fertilized by *fbf-1;fbf-2(RNAi)* sperm are not viable (Luitjens et al., 2000; Thompson et al., 2005). We suggest that defective synapsis is caused by premature expression of the SC proteins. In premeiotic germ cells (and when expressed ectopically in embryonic cells), SC proteins form aggregates. Aggregation might be a conserved property of

synaptonemal proteins, as the yeast and mammalian functional homologs of SYP-2 and SYP-3 have also been reported to aggregate (Ollinger et al., 2005; Sym and Roeder, 1995; Yuan et al., 1996). SC aggregates could reduce the pool of SC proteins available to form SCs and cause synapsis and meiotic chromosomal segregation to fail. We suggest that parallel regulation by FBF of the SC proteins and of meiotic entry regulators (such as GLD-1) reduces non-productive SC aggregation by linking SC synthesis to the production of synapsis-competent chromosomes. We note, however, that not all SC proteins appear to be regulated by FBF. For example, HTP-3 and REC-8 have been detected on chromosomes throughout the mitotic zone (Goodyer et al., 2008; Pasierbek et al., 2001) and do not show obvious regulation by FBF in our 3′ UTR reporter analysis (this study). Also, because FBF is likely to regulate hundreds of mRNAs (Kershner and Kimble, 2010), we cannot exclude the possibility that failed synapsis in *fbf-1;fbf-2* mutants is caused by the misregulation of other proteins besides those analyzed here.

In the absence of FBF, we detected SC protein expression as early as the L2 stage. Premature SC protein expression does not appear to interfere with the proliferation of larval germ cells, as *fbf-1;fbf-2* L4 larvae have normal germ cell numbers (Crittenden et al., 2002). At 25°C, *fbf-1;fbf-2* mutants even maintained mitotic cells into adulthood. *fbf-1;fbf-2* mitotic zones, however, were smaller than in wild type and eventually degenerated in older adults (see Fig. S4 in the supplementary material). These observations suggest that accumulation of meiotic proteins in proliferating germ cells eventually erodes cell renewal and cell viability. One possibility is that true germline stem cells are never formed in *fbf-1;fbf-2* mutants. Instead, descendents of the primordial germ cells differentiate directly at the L2 stage into a premeiotic transitional fate that is characteristic of cells normally found in the second half of the mitotic zone. These 'transit-amplifying' cells retain proliferative potential and the ability to respond to niche signals that balance mitosis and meiosis, but have lost the ability to self-renew for extended periods of time and at all temperatures.

Coordinate regulation of meiosis genes by post-transcriptional mechanisms: parallels between *C. elegans* and mouse

The regulation of meiotic gene expression is best understood in *S. cerevisiae*, in which a transcriptional cascade controls the temporally staggered expression of six classes of meiosis genes (Chu et al., 1998; Kassir et al., 2003; Primig et al., 2000). At the top of the cascade is the master regulator Ime1. Ime1 is a transcription factor that directly activates the transcription of early meiosis genes, including genes required for premeiotic DNA replication and genes required for homolog pairing, such as the yeast homolog of HIM-3/HTP-1/HTP-2 (Kassir et al., 2003). Thus, in yeast, synaptonemal protein expression is also coordinated with meiotic entry, but regulation occurs at the level of transcription. By contrast, in mice, post-transcriptional mechanisms have been implicated in the regulation of early meiotic genes. The RNA-binding proteins DAZL and CPEB (cytoplasmic polyadenylation element binding protein) are both required to promote the expression of the lateral element synaptonemal protein SYCP3 (Reynolds et al., 2007; Tay and Richter, 2001). DAZL and CPEB bind directly to the *Sycp3* 3′ UTR to stimulate its translation (Reynolds et al., 2007; Reynolds et al., 2005; Tay and Richter, 2001). Interestingly, DAZL is also required to activate STRA8, a cytoplasmic activator of meiotic S phase (Lin et al., 2008). In *Stra8* mutants, SYCP3 is expressed but does not load onto chromosomes, similar to what we observe for *C. elegans* SC proteins in the mitotic zone (Anderson et al., 2008). Together, these observations suggest that in mouse, as in *C. elegans*, post-transcriptional mechanisms coordinate the expression of synaptonemal proteins with that of meiotic activators (STRA8 in mouse and GLD-1 in *C. elegans*). One intriguing possibility is that mRNAs activated by DAZL and CPEB are silenced in immature germ cells by FBF-like repressors. Consistent with this possibility, the mammalian FBF homolog PUM2 is expressed in undifferentiated germ cells and has been reported to interact with DAZL (Moore et al., 2003; Xu et al., 2007). It will be interesting to investigate whether mouse meiotic mRNAs are transcribed in immature germ cells but kept silenced by PUM2/FBF, as we have shown here for *C. elegans*.

Competing interests statement
The authors declare no competing financial interests.

Supplementary material
Supplementary material for this article is available at
http://dev.biologists.org/lookup/suppl/doi:10.1242/dev.050799/-/DC1

References
Ahringer, J. and Kimble, J. (1991). Control of the sperm-oocyte switch in Caenorhabditis elegans hermaphrodites by the fem-3 3′ untranslated region. *Nature* **349**, 346-348.

Anderson, E. L., Baltus, A. E., Roepers-Gajadien, H. L., Hassold, T. J., de Rooij, D. G., van Pelt, A. M. and Page, D. C. (2008). Stra8 and its inducer, retinoic acid, regulate meiotic initiation in both spermatogenesis and oogenesis in mice. *Proc. Natl. Acad. Sci. USA* **105**, 14976-14980.

Bailey, T. L. and Elkan, C. (1994). Fitting a mixture model by expectation maximization to discover motifs in biopolymers. *Proc. Int. Conf. Intell. Syst. Mol. Biol.* **2**, 28-36.

Bernstein, D., Hook, B., Hajarnavis, A., Opperman, L. and Wickens, M. (2005). Binding specificity and mRNA targets of a C. elegans PUF protein, FBF-1. *RNA* **11**, 447-458.

Bhalla, N., Wynne, D. J., Jantsch, V. and Dernburg, A. F. (2008). ZHP-3 acts at crossovers to couple meiotic recombination with synaptonemal complex disassembly and bivalent formation in C. elegans. *PLoS Genet.* **4**, e1000235.

Brenner, S. (1974). The genetics of Caenorhabditis elegans. *Genetics* **77**, 71-94.

Byrd, D. T. and Kimble, J. (2009). Scratching the niche that controls Caenorhabditis elegans germline stem cells. *Semin. Cell Dev. Biol.* **20**, 1107-1113.

Cheeseman, I. M., Niessen, S., Anderson, S., Hyndman, F., Yates, J. R., 3rd, Oegema, K. and Desai, A. (2004). A conserved protein network controls assembly of the outer kinetochore and its ability to sustain tension. *Genes Dev.* **18**, 2255-2268.

Chu, S., DeRisi, J., Eisen, M., Mulholland, J., Botstein, D., Brown, P. O. and Herskowitz, I. (1998). The transcriptional program of sporulation in budding yeast. *Science* **282**, 699-705.

Cinquin, O., Crittenden, S. L., Morgan, D. E. and Kimble, J. (2010). Progression from a stem cell-like state to early differentiation in the C. elegans germ line. *Proc. Natl. Acad. Sci. USA* **107**, 2048-2053.

Ciosk, R., DePalma, M. and Priess, J. R. (2004). ATX-2, the C. elegans ortholog of ataxin 2, functions in translational regulation in the germline. *Development* **131**, 4831-4841.

Colaiacovo, M. P., MacQueen, A. J., Martinez-Perez, E., McDonald, K., Adamo, A., La Volpe, A. and Villeneuve, A. M. (2003). Synaptonemal complex assembly in C. elegans is dispensable for loading strand-exchange proteins but critical for proper completion of recombination. *Dev. Cell* **5**, 463-474.

Couteau, F. and Zetka, M. (2005). HTP-1 coordinates synaptonemal complex assembly with homolog alignment during meiosis in C. elegans. *Genes Dev.* **19**, 2744-2756.

Couteau, F., Nabeshima, K., Villeneuve, A. and Zetka, M. (2004). A component of C. elegans meiotic chromosome axes at the interface of homolog alignment, synapsis, nuclear reorganization, and recombination. *Curr. Biol.* **14**, 585-592.

Crittenden, S. L., Bernstein, D. S., Bachorik, J. L., Thompson, B. E., Gallegos, M., Petcherski, A. G., Moulder, G., Barstead, R., Wickens, M. and Kimble, J. (2002). A conserved RNA-binding protein controls germline stem cells in Caenorhabditis elegans. *Nature* **417**, 660-663.

Goodyer, W., Kaitna, S., Couteau, F., Ward, J. D., Boulton, S. J. and Zetka, M. (2008). HTP-3 links DSB formation with homolog pairing and crossing over during C. elegans meiosis. *Dev. Cell* **14**, 263-274.

Hajarnavis, A., Korf, I. and Durbin, R. (2004). A probabilistic model of 3′ end formation in Caenorhabditis elegans. *Nucleic Acids Res.* **32**, 3392-3399.

Hansen, D., Hubbard, E. J. and Schedl, T. (2004). Multi-pathway control of the proliferation versus meiotic development decision in the Caenorhabditis elegans germline. *Dev. Biol.* **268**, 342-357.

Hubbard, E. J. (2007). Caenorhabditis elegans germ line: a model for stem cell biology. *Dev. Dyn.* **236**, 3343-3357.

Jones, A. R., Francis, R. and Schedl, T. (1996). GLD-1, a cytoplasmic protein essential for oocyte differentiation, shows stage- and sex-specific expression during Caenorhabditis elegans germline development. *Dev. Biol.* **180**, 165-183.

Kamath, R. S., Fraser, A. G., Dong, Y., Poulin, G., Durbin, R., Gotta, M., Kanapin, A., Le Bot, N., Moreno, S., Sohrmann, M. et al. (2003). Systematic functional analysis of the Caenorhabditis elegans genome using RNAi. *Nature* **421**, 231-237.

Kassir, Y., Adir, N., Boger-Nadjar, E., Raviv, N. G., Rubin-Bejerano, I., Sagee, S. and Shenhar, G. (2003). Transcriptional regulation of meiosis in budding yeast. *Int. Rev. Cytol.* **224**, 111-171.

Kershner, A. M. and Kimble, J. (2010). Genome-wide analysis of mRNA targets for Caenorhabditis elegans FBF, a conserved stem cell regulator. *Proc. Natl. Acad. Sci. USA* **107**, 3936-3941.

Lamont, L. B., Crittenden, S. L., Bernstein, D., Wickens, M. and Kimble, J. (2004). FBF-1 and FBF-2 regulate the size of the mitotic region in the C. elegans germline. *Dev. Cell* **7**, 697-707.

Lee, M. H., Hook, B., Lamont, L. B., Wickens, M. and Kimble, J. (2006). LIP-1 phosphatase controls the extent of germline proliferation in Caenorhabditis elegans. *EMBO J.* **25**, 88-96.

Lin, Y., Gill, M. E., Koubova, J. and Page, D. C. (2008). Germ cell-intrinsic and -extrinsic factors govern meiotic initiation in mouse embryos. *Science* **322**, 1685-1687.

Luitjens, C., Gallegos, M., Kraemer, B., Kimble, J. and Wickens, M. (2000). CPEB proteins control two key steps in spermatogenesis in C. elegans. *Genes Dev.* **14**, 2596-2609.

MacQueen, A. J., Colaiacovo, M. P., McDonald, K. and Villeneuve, A. M. (2002). Synapsis-dependent and -independent mechanisms stabilize homolog pairing during meiotic prophase in C. elegans. *Genes Dev.* **16**, 2428-2442.

Martinez-Perez, E., Schvarzstein, M., Barroso, C., Lightfoot, J., Dernburg, A. F. and Villeneuve, A. M. (2008). Crossovers trigger a remodeling of meiotic

chromosome axis composition that is linked to two-step loss of sister chromatid cohesion. *Genes Dev.* **22**, 2886-2901.

Merritt, C., Rasoloson, D., Ko, D. and Seydoux, G. (2008). 3′ UTRs are the primary regulators of gene expression in the C. elegans germline. *Curr. Biol.* **18**, 1476-1482.

Mlynarczyk-Evans, S. and Villeneuve, A. M. (2010). Homologous chromosome pairing and synapsis during oogenesis. In *Oogenesis: the Universal Process* (ed. M.-H. Verlhac and A. Villeneuve), pp. 117-140. Chichester, UK: Wiley-Blackwell.

Moore, F. L., Jaruzelska, J., Fox, M. S., Urano, J., Firpo, M. T., Turek, P. J., Dorfman, D. M. and Pera, R. A. (2003). Human Pumilio-2 is expressed in embryonic stem cells and germ cells and interacts with DAZ (Deleted in AZoospermia) and DAZ-like proteins. *Proc. Natl. Acad. Sci. USA* **100**, 538-543.

Ollinger, R., Alsheimer, M. and Benavente, R. (2005). Mammalian protein SCP1 forms synaptonemal complex-like structures in the absence of meiotic chromosomes. *Mol. Biol. Cell* **16**, 212-217.

Pasierbek, P., Jantsch, M., Melcher, M., Schleiffer, A., Schweizer, D. and Loidl, J. (2001). A Caenorhabditis elegans cohesion protein with functions in meiotic chromosome pairing and disjunction. *Genes Dev.* **15**, 1349-1360.

Pfaffl, M. W. (2001). A new mathematical model for relative quantification in real-time RT-PCR. *Nucleic Acids Res.* **29**, e45.

Phillips, C. M. and Dernburg, A. F. (2006). A family of zinc-finger proteins is required for chromosome-specific pairing and synapsis during meiosis in C. elegans. *Dev. Cell* **11**, 817-829.

Praitis, V., Casey, E., Collar, D. and Austin, J. (2001). Creation of low-copy integrated transgenic lines in Caenorhabditis elegans. *Genetics* **157**, 1217-1226.

Primig, M., Williams, R. M., Winzeler, E. A., Tevzadze, G. G., Conway, A. R., Hwang, S. Y., Davis, R. W. and Esposito, R. E. (2000). The core meiotic transcriptome in budding yeasts. *Nat. Genet.* **26**, 415-423.

Reynolds, N., Collier, B., Maratou, K., Bingham, V., Speed, R. M., Taggart, M., Semple, C. A., Gray, N. K. and Cooke, H. J. (2005). Dazl binds in vivo to specific transcripts and can regulate the pre-meiotic translation of Mvh in germ cells. *Hum. Mol. Genet.* **14**, 3899-3909.

Reynolds, N., Collier, B., Bingham, V., Gray, N. K. and Cooke, H. J. (2007). Translation of the synaptonemal complex component Sycp3 is enhanced in vivo by the germ cell specific regulator Dazl. *RNA* **13**, 974-981.

Smolikov, S., Eizinger, A., Schild-Prufert, K., Hurlburt, A., McDonald, K., Engebrecht, J., Villeneuve, A. M. and Colaiacovo, M. P. (2007). SYP-3 restricts synaptonemal complex assembly to bridge paired chromosome axes during meiosis in Caenorhabditis elegans. *Genetics* **176**, 2015-2025.

Suh, N., Crittenden, S. L., Goldstrohm, A., Hook, B., Thompson, B., Wickens, M. and Kimble, J. (2009). FBF and its dual control of gld-1 expression in the Caenorhabditis elegans germline. *Genetics* **181**, 1249-1260.

Sym, M. and Roeder, G. S. (1995). Zip1-induced changes in synaptonemal complex structure and polycomplex assembly. *J. Cell Biol.* **128**, 455-466.

Tay, J. and Richter, J. D. (2001). Germ cell differentiation and synaptonemal complex formation are disrupted in CPEB knockout mice. *Dev. Cell* **1**, 201-213.

Thompson, B. E., Bernstein, D. S., Bachorik, J. L., Petcherski, A. G., Wickens, M. and Kimble, J. (2005). Dose-dependent control of proliferation and sperm specification by FOG-1/CPEB. *Development* **132**, 3471-3481.

Xu, E. Y., Chang, R., Salmon, N. A. and Reijo Pera, R. A. (2007). A gene trap mutation of a murine homolog of the Drosophila stem cell factor Pumilio results in smaller testes but does not affect litter size or fertility. *Mol. Reprod. Dev.* **74**, 912-921.

Yuan, L., Brundell, E. and Hoog, C. (1996). Expression of the meiosis-specific synaptonemal complex protein 1 in a heterologous system results in the formation of large protein structures. *Exp. Cell Res.* **229**, 272-275.

Zetka, M. C., Kawasaki, I., Strome, S. and Muller, F. (1999). Synapsis and chiasma formation in Caenorhabditis elegans require HIM-3, a meiotic chromosome core component that functions in chromosome segregation. *Genes Dev.* **13**, 2258-2270.

Zhang, B., Gallegos, M., Puoti, A., Durkin, E., Fields, S., Kimble, J. and Wickens, M. P. (1997). A conserved RNA-binding protein that regulates sexual fates in the C. elegans hermaphrodite germ line. *Nature* **390**, 477-484.

Zhu, D., Stumpf, C. R., Krahn, J. M., Wickens, M. and Hall, T. M. (2009). A 5′ cytosine binding pocket in Puf3p specifies regulation of mitochondrial mRNAs. *Proc. Natl. Acad. Sci. USA* **106**, 20192-20197.